NASARAWA STATE UNIVERSITY

KNOWLEDGE FOR DEVELOPMENT

JOURNAL OF SCIENCE, TECHNOLOGY AND EDUCATION (JSTE)

A PUBLICATION OF THE DEPARTMENT OF SCIENCE, TECHNOLOGY & MATHEMATICS EDUCATION (STME), NASARAWA STATE UNIVERSITY, KEFFI

VOLUME 9

ISSN: 2651-5539

JOURNAL OF SCIENCE, TECHNOLOGY AND EDUCATION (JSTE) VOL. 9. NO. 10

JSTE PUBLICATIONS, 2024 www.nsukjste.com/

ISSN: 2651-5539

DRYING KINETICS OF *ANACARDIUM OCCIDENTALE L.* WOOD: COMPARATIVE THIN LAYER AND ARTIFICIAL NEURAL NETWORK MODELING

[1]Areghan S.E and [2]Adeyi A.J*

[1,2]Department of Forest Product Development and Utilization
Forestry Research Institute of Nigeria, Ibadan
P.M.B. 5054
Corresponding Email: adeyi.abiola@yahoo.com

Citation: Areghan S. E & Adeyi A. J. (2025). Drying kinetics of *Anacardium occidentale L.* wood: Comparative thin layer and artificial neural network modeling, Nigeria. *Journal of Science, Technology, and Education (JSTE)*; www.nsukjste.com/ *9*(10), 123-136

Abstract

This study investigated the drying kinetics of *Anacardium occidentale L.* wood using convective drying method and comparative modeling approach. Wood samples of 3 mm and 5 mm thickness were dried at 70, 80, and 100 °C, and their moisture ratios monitored. Traditional thin-layer drying models, including the Logarithmic, Page, and Henderson models, and artificial intelligent model (that is, artificial neural network) were utilized to predict the drying characteristics with statistically evaluations. Results showed that drying progressed in single falling rate period, while higher temperature and reduced thickness increased drying rate. The effective moisture diffusivity increased with temperature, while the activation energy was found to be 22.9 kJ/mol for 5 mm samples and 10.1 kJ/mol for 3 mm samples. The Logarithmic model, achieving an R^2 of up to 0.9995 and RMSE as low as 0.0056, performed best amongst traditional thin layer models. Artificial neural network model yielded an R^2 value of 0.9998, thereby demonstrating overall superior predictive accuracy. These results demonstrated the potential of integrating AI-based models to optimize drying processes in wood processing applications.

Keywords: *Anacardium occidentale L.,* Modelling, Thin Layer, Drying, Artificial Neural Networks

Introduction

Anacardium occidentale L. is a tropical tree with utilization covering economic, industrial, and medicinal applications (Adeigbe *et al.,* 2015). Its wood is valued for its durability and resistance to termite attacks, making it suitable for various applications. In Cambodia, the timber is

employed in boat-making and house construction, while the wood serves as an excellent source of charcoal (Dy Phon, 2000). Similarly, in Nigeria, *Anacardium occidentale L.* wood is utilized for furniture and fishing boats, highlighting its versatility (Adeigbe *et al.,* 2015). The post fruit-active years of cash-crop such as *Anacardium occidentale L.* tree implied its utilization for furniture, firewood, wood gas and others. However, this utilization can only be effective after prior drying of the tree wood products. Hence, this study focuses at determination of drying characteristics of post *Anacardium occidentale L.* tree utilization.

Drying is a **simultaneous heat and mass transfer operation or process** aimed at reducing the moisture content of a material to a desired level (Gandía *et al.,* 2024; Chanpet *et al.,* 2020). It is a fundamental post harvest operation required for a number of applications, such as **preservation of agricultural products and foodstuffs**, thus, enhancing their shelf stability through inhibition of microbial growth and enzymatic activity (Kohli *et al.,* 2022; Mbegbu *et al.,* 2021). In fibrous materials such as wood, drying improves stability, strength, and suitability for various end uses (Du *et al.,* 2005; Zlatanović *et al.,* 2017).

The efficiency and effectiveness of drying processes are governed by a complex interaction of factors related to the type and size of material in question, the surrounding environment during drying processing, and the type of drying method employed (Zlatanović *et al.,* 2017; Mascarenhas *et al.,* 2023); hence drying processes require rigorous investigation. Due to enormous cost and time resources requirements, drying processes are investigated, designed, experimented, and analyzed in laboratory scale, serving as a background to up-scaling for industrial utilization.

The kinetics of drying are typically described by the change in moisture content over time, often represented through a **drying curve** (Omolola *et al.,* 2019; Kohli *et al.,* 2022). These curves exhibit distinct phases, including an initial adjustment period, a **constant rate period (CRP)** where moisture evaporates readily from the surface, and one or more **falling rate periods (FRP)** where the rate of moisture removal is controlled by the internal resistance to moisture movement (Gandía *et al.,* 2024; Chanpet *et al.,* 2020). The transition between these periods is caused by factors such as air velocity, with higher velocities leading to a faster transition (Chanpet *et al.,* 2020). The rate of internal moisture transfer is characterized by the **effective moisture diffusivity (**D_{exp}**)**, a

temperature-dependent parameter that generally increases with temperature following the **Arrhenius equation** (Kohli *et al.,* 2018). The **activation energy (E_a)** derived from this relationship quantifies the energy barrier for moisture diffusion (Omolola *et al.,* 2019).

To understand the drying kinetics for process and equipment design purposes, **modeling** serves an indispensable tool (Gandía *et al.,* 2024; Sridhar & Madhu 2015). Mathematical models, such as various **thin-layer drying models**, ranging from simple empirical equations to more complex semi-theoretical and theoretical models, are applied to describe the relationship between moisture ratio and drying time (Sridhar & Madhu, 2015). Models such as the **Page model** (Kohli *et al.,* 2022; Zlatanović *et al.,* 2017) and the **Logarithmic model** (Mbegbu *et al.,* 2021) have shown good agreement with experimental data for different agricultural and wood materials. For wood, models based on **Fick's second law of diffusion** are particularly relevant for falling rate period, where internal moisture movement is the rate-limiting step (Weng *et al.,* 2021; Wannadhari *et al.,* 2014).

In furtherance to traditional thin layer drying models, the improved accuracy, real time monitoring capability, versatility and ease of implementation is nowadays encouraging the utilization of artificial intelligent (AI) methods for modeling purposes. Several of AI methods, such as Artificial Neural Networks (ANN), Fuzzy Inference Systems (FIS), Support Vector Machine (SVM), Adaptive Neuro Fuzzy Inference System (ANFIS), and others have been utilized in drying kinetics modelling, with reported better efficiencies over traditional modelling methods (Okonkwo *et al.,* 2023; Ojediran *et al.,* 2021). Therefore, it is in order to compare selected traditional thin layer drying models with selected artificial intelligent modelling strategies to predict the drying kinetics for optimal performances.

Continued research into drying kinetics, particularly the development of adaptable models (Gandía *et al.,* 2024) and sensitivity analysis remain a significant area of scientific and technological importance. Therefore, this study aimed at investigating the drying characteristics of *Anacardium occidentale L.* wood, determine the occurring drying mechanisms and comparatively model the drying characteristics with traditional thin layer models and ANN model to assist utilization, dryer or process design and enhanced drying or process control.

Materials and Methods

Materials

Anacardium occidentale L. sample was

obtained from a sawmill in Ogbomoso, Oyo State, Nigeria, and served as the experimental material. A Stangas convective oven, equipped with a temperature regulator, a 3.0 kW heating element, and a timer, was used for the drying experiments. A digital weighing balance with a precision of 0.001 g measured the weight of each sample. The samples were saw into 5 mm x 5 mm x 5 mm, and 5 mm x 5 mm x 3 mm, and their dimensions were confirmed using a Vernier caliper.

Drying Experiment

The initial moisture content of the wood sample was determined using the AOC (1990) method by drying 30 g of the sample in the convective oven at 105 ^{O}C for 24 h. The experiment was designed to test the effect of temperature (70, 80 and 90^{O}C) and sample thickness (2 and 5 mm) on the drying characteristics of *Anacardium occidentale L. in accordance with the methods of* Sridhar & Madhu (2015) and Adeyi *et al.,* (2020*).* The oven run for 20 min at a set temperature and constant air velocity (1 m/s^2) prior to samples introduction. The initial and hourly weight of the sample for 10 h was recorded using weighing balance. Moisture content, moisture ratio, EMD and activation energy (Eqn 1 - 4) were determined from the instantaneous weight record and initial moisture content of the sample using Matlab 2010a software.

$$M_a(d.b) = \frac{W_F - W_D}{W_D} X\ 100\% \quad (1)$$

$$MR = \frac{M_t - M_e}{M_a - M_e} \quad (2)$$

$$Ln\ MR = Ln(\frac{8}{\pi^2}) - \frac{D_{exp}}{4\ L^2}\pi^2 t \quad (3)$$

$$D_{exp} = D_0\ exp\left[\frac{E_a}{RT}\right] \quad (4)$$

Where M_a = initial moisture content in percentage dry basis (%), W_F = fresh weight of the sample (g) and W_D = dried weight of the sample (g), M_t = moisture content at a given time t during drying (g of water/g of dry matter) and M_e = final equilibrium moisture content (g of water/g of dry mater), D_{eff} is the EMD (m^2/s), L is the half thickness of the product (m), and t is drying time (s). The EMD is therefore the slope of the straight line obtained by plotting natural logarithm of moisture ratio against drying time.

The solution of Eqn. 3 and 4, to determine D_{exp} and $E_a$can be found elsewhere (Sridhar & Madhu 2015; Adeyi *et al.,* 2020; Mbegbu *et al.,* 2021; Kohli *et al.,* 2022).

Thin Layer Modeling **Six thin layer models were utilized to fit the drying characteristics data using Matlab 2010 software. The models names and their respective mathematical composition are represented in Table 2.**

Table 2: Semi-empirical Models

Model Name	Model Equation	Number	Reference
Lewis	**MR = exp (-k*t)**	**5**	**Adeyi (2024)**
Page	MR = exp ($-k*t^n$)	6	**Adeyi (2024)**
Logarithmic	MR = a*exp (-k*t) + c	7	**Adeyi (2024)**
Henderson	MR = a e^{-ktn}	8	Kohli *et al.,* (2022)
Midilli	MR = a e^{-kt} + b t	9	Kohli *et al.,* (2022)
Peleg	MR = 1 - $\frac{t}{(a+bt)}$	10	Kohli *et al.,* (2022)

ANN Modelling

The data-set was constructed to model the drying process using three input parameters, Time (h), Temperature (°C), and Thickness (mm). The output variable, Moisture Ratio (MR), was recorded for six experimental configurations (combinations of Temperature and Thickness) with time-series data (0 to 9 hours). The data-set was organized such that each experimental condition contributed 10 data points, resulting in a total of 60 observations.

An ANN was designed with the following characteristics; Input Layer consisting of 3 neurons corresponding to the three input factors, Hidden Layers consisting of Two hidden layers with 10 and 5 neurons, respectively, using the tansig activation function, and Output Layer consisting of a single neuron with a purelin activation function to predict MR. Training Algorithm: The network was trained using the Levenberg–Marquardt algorithm (trainlm) with specified training parameters (that is, maximum epochs = 1000, training goal MSE = 1e-6). The ANN was trained on the complete dataset and evaluated using statistical measure to ensure adequate model performance.

Modelling Efficiency

Model performance was evaluated using the sum of squared error (SSE), coefficient of determination (R^2), and root mean square error (RMSE). Lower SSE and RMSE, along with a higher R^2 (ranging from 0 to 1), indicate a better model fit. Eqns. 11 – 13 define these metrics, where predictions are compared against experimental values.

$$SSE = \sum_{i=1}^{n}(Pred,i - Exp,i)^2 \qquad (11)$$

$$R^2 = 1 - \left(\sum_{i=1}^{n} \frac{(Pred,i - Exp,i)^2}{(Pred,i - AverageExp)^2}\right) \qquad (12)$$

$$RMSE = \sqrt{\frac{\sum_{i=1}^{n}(Exp,i - Pred,i)^2}{N}} \qquad (13)$$

Where, Pred,i is the i_{th} predicted value, Exp,i is the ith experimental value and AveragedExp is the average of all the experimental value. n represents the number of observations.

Results and Discussions

The initial moisture content of *Anacardium occidentale wood utilized in this study was 48.9% (d.b). The drying curve of the samples (3 and 5 mm) at varied temperature (70, 80 and 100 ^{O}C) are represented in Fig. 1. The drying curve indicated a single rate period, which is common to most agricultural and food material (Adeyi* et al., *2023).*

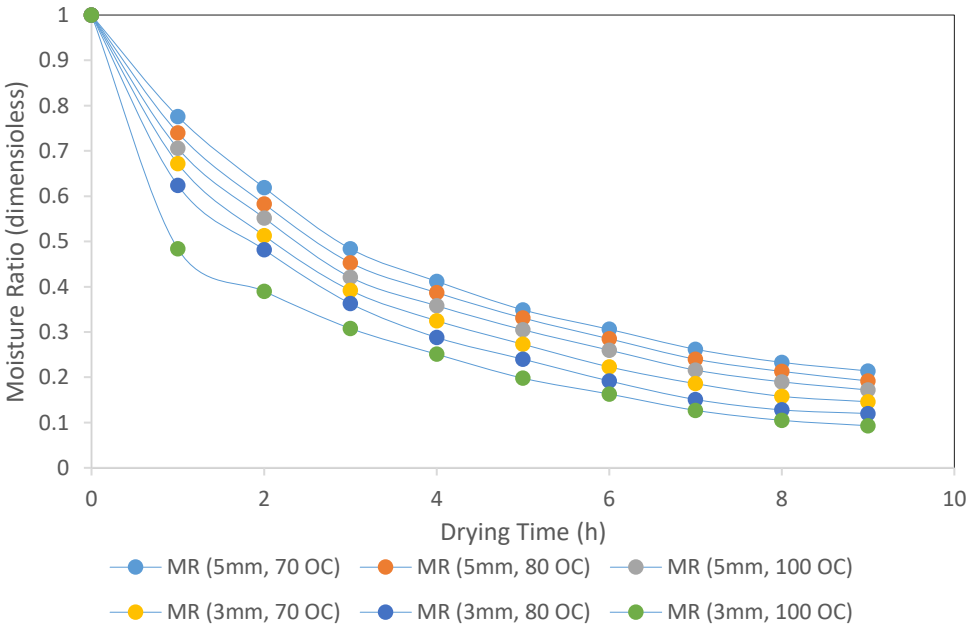

Fig. 1: Drying Curve of *Anacardium occidentale Wood*

The curves indicates that, for a given sample thickness (that is 5 or 3 mm), higher drying temperatures resulted in faster decrease in the moisture ratio (MR). This is attributed to factors such as i**ncreased vapor pressure gradient, where** at higher temperatures, water vapor pressure within the product increases, thus enhancing the driving force for moisture diffusion from the interior to the surface of the material (Mbegbu *et al.,* 2021). In addition, the curve showed that the constant-rate period is shortened as temperature increases, allowing the process to transition more quickly to the falling-rate period. The figure confirmed that samples dried at 100 °C reached the lowest moisture ratios at any given time compared to those dried at 70 °C or 80 °C, emphasizing the well-known direct relationship between drying temperature and drying rate (Adeyi *et al.,* 2023; Sridhar & Madhu 2015).

Comparing drying curves for 3 mm and 5 mm thicknesses at the same temperature showed that thinner samples (3 mm) exhibited a faster decrease in MR. This is explained by the fact that thinner samples have less distance for moisture to diffuse from the interior to the surface compared to thicker samples, leading to a higher effective diffusion rate. More also in thinner samples, heat can penetrate more easily, maintaining a higher temperature throughout the sample and accelerating moisture removal. Furthermore, thinner slices generally have a higher surface area relative to their volume, promoting more efficient mass (moisture) transfer to the surrounding environment. Hence, at any given drying time and temperature, the 3 mm slices showed lower moisture ratios than the 5 mm slices. Similar result was observed for different thicknesses of unripe plantain during oven drying (Adeyi *et al.,* 2022).

Thin Layer Model Efficiency

The parameters and efficiency of the employed thin layer models in this study are summarized in Table 1. The performance of each model was statistically evaluated using SSE, R^2, and RMSE.

Table 1: Performances of the Thin Layer Models

(a) Data set: 5mm, 70°C

Model	Fitted Parameters (xFit)	SSE	R^2	RMSE
Lewis	k = 0.2073	0.0129	0.9787	0.0359
Page	k = 0.2829, n = 0.7991	0.0018	0.9971	0.0133
Logarithmic	a = 0.8327, k = 0.3078, c = 0.1656	0.0003	0.9995	0.0056
Henderson	a = 1.0066, k = 0.2882, n = 0.7920	0.0017	0.9972	0.0131
Midilli	a = 0.9944, k = 0.2595, b = 0.0140	0.0006	0.9990	0.0076
Peleg	a = 3.3249, b = 0.8861	0.0007	0.9988	0.0085

(b) Data set: 5mm, 80°C

Model	Fitted Parameters (xFit)	SSE	R^2	RMSE
Lewis	k = 0.2251	0.0176	0.9714	0.0420
Page	k = 0.3236, n = 0.7601	0.0010	0.9983	0.0101
Logarithmic	a = 0.8274, k = 0.3375, c = 0.1634	0.0010	0.9984	0.0100
Henderson	a = 1.0042, k = 0.3270, n = 0.7561	0.0010	0.9984	0.0100
Midilli	a = 0.9850, k = 0.2804, b = 0.0142	0.0017	0.9972	0.0132
Peleg	a = 2.8865, b = 0.9112	0.0003	0.9995	0.0055

(c) Data set: 5mm, 100°C

Model	Fitted Parameters (xFit)	SSE	R^2	RMSE
Lewis	k = 0.2469	0.0218	0.9656	0.0467
Page	k = 0.3647, n = 0.7340	0.0008	0.9987	0.0090
Logarithmic	a = 0.8306, k = 0.3698, c = 0.1560	0.0018	0.9972	0.0134
Henderson	a = 1.0029, k = 0.3671, n = 0.7315	0.0008	0.9987	0.0090
Midilli	a = 0.9794, k = 0.3057, b = 0.0141	0.0029	0.9954	0.0171
Peleg	a = 2.5187, b = 0.9242	0.0003	0.9995	0.0059

(d) Data set: 3mm, 70°C

Model	Fitted Parameters (xFit)	SSE	R^2	RMSE
Lewis	k = 0.2771	0.0229	0.9656	0.0479
Page	k = 0.4079, n = 0.7248	0.0004	0.9994	0.0062
Logarithmic	a = 0.8462, k = 0.3997, c = 0.1367	0.0026	0.9962	0.0160
Henderson	a = 1.0016, k = 0.4092, n = 0.7235	0.0004	0.9994	0.0061
Midilli	a = 0.9751, k = 0.3345, b = 0.0128	0.0039	0.9941	0.0198
Peleg	a = 2.2073, b = 0.9205	0.0003	0.9996	0.0053

(e) Data set: 3mm, 80°C

Model	Fitted Parameters (xFit)	SSE	R^2	RMSE
Lewis	k = 0.3136	0.0249	0.9643	0.0499
Page	k = 0.4608, n = 0.7109	0.0004	0.9994	0.0062
Logarithmic	a = 0.8595, k = 0.4319, c = 0.1170	0.0048	0.9931	0.0220
Henderson	a = 0.9994, k = 0.4602, n = 0.7114	0.0004	0.9994	0.0062
Midilli	a = 0.9681, k = 0.3660, b = 0.0112	0.0065	0.9907	0.0255
Peleg	a = 1.9141, b = 0.9187	0.0011	0.9985	0.0103

(f) Data set: 3mm, 100°C

Model	Fitted Parameters (xFit)	SSE	R^2	RMSE
Lewis	k = 0.3951	0.0626	0.9070	0.0791
Page	k = 0.6728, n = 0.5525	0.0020	0.9970	0.0142
Logarithmic	a = 0.8336, k = 0.6219, c = 0.1322	0.0194	0.9712	0.0440
Henderson	a = 0.9976, k = 0.6704, n = 0.5537	0.0020	0.9970	0.0142
Midilli	a = 0.9445, k = 0.4698, b = 0.0133	0.0263	0.9609	0.0513
Peleg	a = 1.1560, b = 0.9984	0.0061	0.9909	0.0247

In the table, models including Peleg, Logarithmic, Page, and Henderson exhibited the best fit (high R^2, low SSE, RMSE) while the Lewis models consistently showed poor performance. The model parameters (xFit) varied with changes in temperatures and thicknesses, showing the influence of drying conditions on the drying process. The Logarithmic model consistently showed efficiency in fitting various materials dried using different methods, showing its verssatility, for instance, in scent and lemon basil leaves (Mbegbu *et al.,* 2021), basil leaves (Seyedabadi, 2015) and casuarina equisetifolia wood chips (Sridhar & Madhu, 2015). Page models was also identified as a good fit for asparagus roots (Kohli *et al.,* 2018) while Henderson model showed excellent fits for Acacia mangium wood (Wan *et al.,* 2014), a trend also observed in Table 1. In addition, the Lewis model's poor fit in Table 1 is consistent with its general limitations as also noted for *Casuarina equisetifolia* (Sridhar & Madhu, 2015), suggesting its oversimplified nature for complex drying processes.

The parameter k implied drying rate constant (Kohli *et al.,* 2018). In Table 1, k values tend to increase with higher temperatures across most models, implying accelerated drying at elevated temperatures, which is a fundamental principle of drying (Chanpet *et al.,* 2020). The parameter n implying a shape parameter in Page model, accounts for deviations from a simple exponential drying curve and can be related to changes in the internal resistance to moisture transfer over time (Mbegbu *et al.,* 2021). Variations in n with temperature and thickness in Table 1 suggest that the drying mechanism's evolution is influenced by these factors (Kohli *et al.,* 2018). The variability of other parameters across the data sets in Table 1 implied the sensitivity of the model fit to the specific drying conditions.

The drying mechanism of the samples in terms of Diffusion Coefficient and Effective Moisture Diffusivity is represented in Table 2

Table 2: Diffusion Coefficient and Activation Energy of the Samples

Sample Thickness (mm)	D_{exp} (m^2/s) at 70°C	D_{exp} (m^2/s) at 80°C	D_{exp} (m^2/s) at 100°C	Activation Energy (E_a) (kJ/mol)
5 mm	1.127×10^{-10}	1.171×10^{-10}	1.229×10^{-10}	22.9
3 mm	1.349×10^{-10}	1.492×10^{-10}	1.492×10^{-10}	10.1

The table showed that for both sample thicknesses, the **effective diffusivity increases as the temperature rises** from 70°C to 100°C, which aligns with the general understanding that higher temperatures accelerate moisture removal during drying (Chanpet *et al.,* 2020; Sridhar & Madhu, 2015; Mbegbu *et al.,* 2021; Kohli *et al.,* 2022). The a**ctivation energy (Ea), representing the minimum energy needed for moisture diffusion to occur within the material also showed variation across the sample thicknesses.** A **lower Ea value signified that the temperature sensitivity of the effective diffusivity is diminished**. Consequently, for the 3 mm sample, the rate at which effective diffusivity increases with temperature is less pronounced compared to the 5 mm sample within the 70 -100°C range.

Therefore, the **thickness of the material significantly influenced the internal resistance to moisture movement** during drying. In **thicker materials**, moisture has a longer path to travel to reach the surface and evaporate. This internal movement often becomes the rate-limiting factor, particularly during the falling rate period. Overcoming this internal resistance necessitates a greater energy input and leads to a stronger dependence on temperature, thus resulting in a **higher activation energy (**Kohli *et al.,* 2018; Mbegbu *et al.,* 2021). In general, a lower activation energy indicates a weaker dependence of the diffusion process on temperature, which could be attributed to the less significant role of internal diffusion resistance in the thinner sample.

ANN Modeling and Prediction Efficiency

The ANN performance on the drying characteristics is represented in Fig. 2

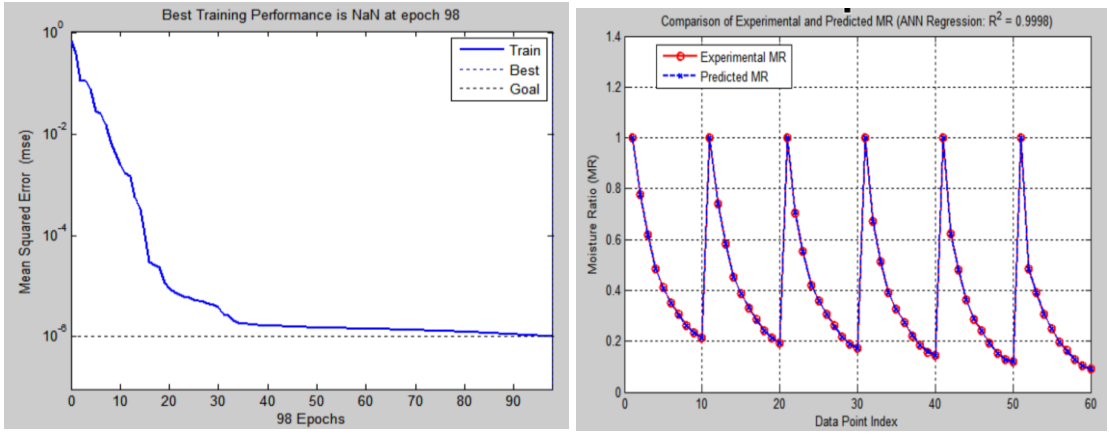

(a) (b)

Fig. 2: (a) Training Performance and (b) Prediction Efficiency of ANN

The training performance in Fig. 1 (a) showed that ANN training progressed efficiently without overfitting as shown by the continued decreasing Mean Squared Error. This lack of overfitting characteristics of the ANN is desirable as it speaks to the fact that ANN structure8 actually understood the existing pattern in the drying data rather and provided predictions rather than memorizing the data. A similar observation was reported by Adeyi *et al.,* (2021). In addition, the converged epoch around 100 epochs showed that the ANN structure was prudent in the utilization of computer memory resources, this is in line with the report of Ojediran *et al.,* (2022).

Furthermore, the modeling efficiency in Fig. 2 (b) showed that ANN structure predicted with R^2 value of 0.9998, which justify the almost perfect fitting observed in the Figure. Compared with all the thin layer model utilized in this study, it is observed that ANN has the highest modeling and prediction efficiency. This confirms the wide observation that intelligent modeling methods tend to show capability in presenting accurate models (Okonkwo *et al.,* 2023).

Conclusion

The effect of drying temperature, and sample thickness on the drying characteristics of *Anacardium occidentale L.* wood. In addition, the drying mechanism and drying characteristics modeling, using mathematical and artificial neural network modeling was investigated. The study concludes that the drying kinetics of *Anacardium occidentale L.* wood are effectively characterized using both traditional thin-layer drying models and an artificial neural network (ANN). While models such as Logarithmic, Page, and Henderson achieved high accuracy (with R^2 values reaching up to 0.9995), the ANN model outperformed them with an R^2 of 0.9998. Additionally, results indicated that higher temperatures significantly enhance the drying rate by increasing the effective moisture diffusivity, and thinner samples exhibit lower activation energies. These results provide valuable background for optimizing drying processes in wood processing applications.

Declaration of Conflict of Interest

The author declares no conflict of interest on this article.

References

Adeigbe, O. O., Olasupo, F. O., Adewale, B. D., & Muyiwa, A. A. (2015). A review on cashew research and production in Nigeria in the last four decades. *Scientific Research and Essays, 10*(5), 196–209. https://doi.org/10.5897/sre2014.5953

Adeyi, A. J. (2024). Drying process of *Senna alata* medicinal leaves: Comparative empirical and artificial neural networks modelling of mass transfer kinetics with energy analysis. *Alexandria Journal of Engineering Research and Development, 7*(2), 139–151. https://doi.org/10.53982/ajerd.2024.0702.14-j

Adeyi, A. J., Adeyi, O., Oke, E. O., Okonkwo, E., & Ogunsola, A. D. (2021). Effective moisture diffusivity of *Sierrathrissa leonensis* cracker: Optimization, sensitivity and uncertainty analyses. *Scientific African, 12*, e00807. https://doi.org/10.1016/j.sciaf.2021.e00807

Adeyi, A. J., Durowoju, M. O., & Adeyi, O. (2018). Experimental studies and artificial neural networks (ANN) modeling of moisture absorption characteristics of polyester/momodical fiber reinforced composite. *International Journal of Mechanical Engineering and Technology, 9*(11), 1453–1467.

Chanpet, M., Rakmak, N., Matan, N., & Siripatana, C. (2020). Effect of air velocity, temperature, and relative humidity on drying kinetics of rubberwood. *Heliyon, 6*(10), e05151. https://doi.org/10.1016/j.heliyon.2020.e05151

Dy Phon, P. (2000). *Plants utilised in Cambodia/Plantes utilisées au Cambodge*. Imprimerie Olympic.

Du, G., Wang, S., & Cai, Z. (2005). Microwave drying of wood strands. *Drying Technology, 23*(12), 2421–2436. https://doi.org/10.1080/07373930500340494

Gandía Ventura, I., Velázquez Martí, B., López Cortes, I., & Guerrero-Luzuriaga, S. (2024). Kinetic models of wood biomass drying in hot airflow systems. *Applied Sciences, 14*(15), 6716. https://doi.org/10.3390/app14156716

Kohli, D., Shahi, N. C., & Kumar, A. (2018). Drying kinetics and activation energy of asparagus root (*Asparagus racemosus* Wild.) for different methods of drying. *Current Research in Nutrition and Food Science Journal, 6*(1), 191–202. https://doi.org/10.12944/crnfsj.6.1.22

Mascarenhas, F. J., Geraldes Dias, A. M., Christoforo, A. L., Santos Simões, R. M., & Cunha, A. E. (2022). Effect of microwave treatment on drying and water impregnableness of *Pinus pinaster* and *Eucalyptus globulus*. *Maderas. Ciencia y tecnología, 25*. https://doi.org/10.4067/s0718-221x2023000100406

Mbegbu, N., Nwajinka, C., & Amaefule, D. (2021). Thin layer drying models and characteristics of scent leaves (*Ocimum gratissimum*) and lemon basil leaves (*Ocimum africanum*). *Heliyon, 7*(1), e05945. https://doi.org/10.1016/j.heliyon.2021.e05945

Ojediran, J. O., Okonkwo, C. E., Adeyi, A. J., Adeyi, O., Olaniran, A. F., George, N. E., & Olayanju, A. T. (2020). Drying characteristics of yam slices (*Dioscorea rotundata*) in a convective hot air dryer: Application of ANFIS in the prediction of drying kinetics. *Heliyon, 6*(3), e03555. https://doi.org/10.1016/j.heliyon.2020.e03555

Okonkwo, C. E., Olaniran, A. F., Adeyi, A. J., Adeyi, O., Ojediran, J. O., Erinle, O. C., Mary, I. Y., & Taiwo, A. E. (2022). Neural network and adaptive neuro-fuzzy inference system modeling of the hot air drying process of orange-fleshed sweet potato. *Journal of Food Processing and Preservation, 46*, e16312. https://doi.org/10.1111/jfpp.16312

Omolola, A. O., Kapila, P. F., & Silungwe, H. M. (2019). Mathematical modeling of drying characteristics of Jew's mallow (*Corchorus olitorius*) leaves. *Information Processing in Agriculture, 6*(1), 109–115. https://doi.org/10.1016/j.inpa.2018.08.003

Seyedabadi, E. (2015). Drying kinetics modelling of basil in microwave dryer. *Agricultural Communications, 3*(4), 37–44.

Sridhar, D., & Madhu, G. M. (2015). Drying kinetics and mathematical modeling of *Casuarina equisetifolia* wood chips at various temperatures. *Periodica Polytechnica Chemical Engineering, 59*(4), 288–295. https://doi.org/10.3311/ppch.7855

Wan Nadhari, W. N., Hashim, R., Danish, M., Sulaiman, O., & Hiziroglu, S. (2014). A model of drying kinetics of *Acacia mangium* wood at different temperatures. *Drying Technology, 32*(3), 361–370. https://doi.org/10.1080/07373937.2013.829855

Zlatanović, I., Pajić, M., Rančić, D., Dajić-Stevanović, Z., & Dudić, D. (2017). Drying kinetics and shrinkage analysis of *Valeriana officinalis* roots. *FME Transactions, 45*(1), 142–148. https://doi.org/10.5937/fmet1701142z